

Computer-Aided Drug Design Studies in Association with *in vitro* Antileishmanial Tests for New Chalcones

Gleice R. da Silva,^a Francisnaira S. Santos,^{id b,c} Fernando F. Leite,^a Chonny A. H. Acevedo,^{id a}
Natália F. de Sousa,^a Gabriela B. Grimaldi,^b Milena B. P. Soares,^{c,d} Elisalva T. Guimarães,^{b,c}
Marcus T. Scotti,^{id a} Luis Cezar Rodrigues,^e Francisco J. B. Mendonça Júnior,^f Eloísa H. Campana,^{id g}
José M. Barbosa Filho,^a Hemerson I. F. Guimarães^{id g,h} and Felipe Q. S. Guerra^{id *,a,g}

^aPrograma de Pós-Graduação em Produtos Naturais e Sintéticos Bioativos,
Centro de Ciências da Saúde, Universidade Federal da Paraíba, 58051-900 João Pessoa-PB, Brazil

^bLaboratório de Histotécnica e Cultura Celular, Departamento de Ciências da Vida,
Universidade do Estado da Bahia, 41150-000 Salvador-BA, Brazil

^cLaboratório de Engenharia Tecidual e Imunofarmacologia, Instituto Gonçalo Moniz,
Fundação Oswaldo Cruz, 40296-710 Salvador-BA, Brazil

^dInstituto Senai de Inovação em Sistemas Avançados em Saúde, SENAI/CIMATEC,
41650-010 Salvador-BA, Brazil

^ePrograma de Pós-Graduação em Desenvolvimento e Inovação Tecnológica em Medicamentos,
Universidade Federal da Paraíba, 58051-900 João Pessoa-PB, Brazil

^fLaboratório de Síntese e Vetorização de Moléculas, Universidade Estadual da Paraíba,
58071-160 João Pessoa-PB, Brazil

^gDepartamento de Ciências Farmacêuticas, Centro de Ciências da Saúde,
Universidade Federal da Paraíba, 58051-900 João Pessoa-PB, Brazil

^hPrograma de Pós-Graduação em Ciências Farmacêuticas, Departamento de Ciências da Vida,
Universidade do Estado da Bahia, 41150-000 Salvador-BA, Brazil

In silico and *in vitro* tests can reveal promising anti-leishmania activity for natural products and their derivatives. The aim of this study was to investigate *in silico* the pharmacological activities of potential new chalcones and their leishmanicidal potential *in vitro*. The *in silico* study was carried out using the PASS, MolPredictX and Molegro Virtual Docker 6.0 programs. Antiparasitic activity was assessed in axenic promastigote and amastigote forms of *Leishmania braziliensis*. The cytotoxicity tests used the J77G8 cell line. The chalcones exhibited 50% cytotoxic concentration values (CC₅₀) values > 50 μM. Chalcone **4** (named FERAI) presented the best activity with concentration for 50% of promastigotes and intracellular parasites forms (EC₅₀) of 9.75 ± 1.7 and 10.13 ± 1.7 μM for promastigote and amastigote, respectively. Reactive oxygen species (ROS) testing presented increased ROS levels in the parasite at the FERAI concentrations of 10 μM (56.33%), 20 μM (61.76%) and 30 μM (67.13%). Molecular docking revealed interactions (binding energy) between FERAI and the enzymes UDP-glycosyl pyrophosphorylase (-56.8384), dihydroorotate-dehydrogenase (-132.276) and trypanothione-reductase (-151.281). Our results demonstrated the anti-leishmanial activity of chalcones, especially FERAI, with a noted raising of ROS levels in the parasite. Molecular docking revealed dihydroorotate dehydrogenase and trypanothione reductase as potential pharmacological targets for FERAI.

Keywords: flavonoids, computer-aided drug design, homology modeling, molecular docking, pharmacological activity, MolPredictX

*e-mail: fqsg@academico.ufpb.br

Editor handled this article: Paula Homem-de-Mello (Associate)



Introduction

Computer-aided drug design has emerged as a powerful tool with an important role to play in the development of new therapeutic molecules. Structure-based and ligand-based drug design are frequently employed in computer-aided drug design.¹ Computational methods complement *in vitro* and *in vivo* pharmacological testing, potentially reducing costs, experimental time, and even the necessity for animal tests, while enhancing predictive accuracy and safety.^{2,3}

Great evolution has taken place in the area of *in silico* drug discovery over the last decade. This space now provides a more targeted and precise approach compared to those of the past, which often required the discovery and identification of active molecules that would subsequently undergo numerous tests in order to be targeted.^{4,5} *In silico* analyses provide a powerful tool: the ability to quantitatively predict the activity of compounds and simultaneously study interactions between a test substance and its targets, such as proteins. The combination allows for a more complete understanding of pharmacological activity, as it takes into account binding to specific target proteins.⁶⁻⁸

Research with natural products and novel synthetic substances exploits these tools to reach new levels of efficiency and time optimization, providing safer and more reliable results. In this sense, in order to increase knowledge about the therapeutic potential of natural compounds, *in silico* studies are being carried out on various chemical classes, including alkaloids, terpenes, flavonoids and others, all with the aim of obtaining more precise and targeted results.⁹⁻¹²

Flavonoids are polyphenolic phytochemical compounds found in many plants, fruits, vegetables and leaves with frequent applications in medicinal chemistry. In the field of scientific research, these compounds stand out for having a wide range of *in vitro* and *in vivo* pharmacological activity, making them potential candidates for the development of new therapies. Anticancer, antioxidant, anti-inflammatory, antiviral and antileishmanial properties have already been reported in the literature for these compounds.^{13,14}

In terms of anti-leishmania activity, both natural and synthetic flavonoid compounds have been shown to inhibit parasites. Synthetic derivatives have proven activity against amastigote forms of *Leishmania braziliensis*, eliminating the parasite from mammalian host cells, and demonstrating its pharmacological safety.¹⁵ Dehydrolupinifolinol and sericetin (derived from *Mundulea sericea*) have been shown to be active against drug-sensitive *L. donovani*. Other natural flavonoids as well have presented antileishmanial activity against *L. mexicana*, *L. major*, and *L. braziliensis*.¹⁶⁻¹⁹

Chalcones are secondary metabolites found in edible and medicinal plants. In the plant kingdom, chalcones play a fundamental role as flavonoid bio-precursors, acting as important intermediaries in the biosynthetic pathway. Chalcones possess a range of pharmacological activities, such as antioxidant, anticancer, antimicrobial, antiviral, anti-plasmodic, and (like flavonoids) antileishmanial.²⁰

In Brazil, the first compounds used to treat leishmaniasis were antimonials, followed by pentavalent derivatives (Sb⁵⁺), which are still used today. Antimoniato-*N*-methyl glucamine is the drug of choice for treatment of tegumentary and visceral leishmaniasis.¹⁵ In cases of resistance or contraindication, amphotericin B can also be used. The biggest problems involved when using such drugs are their high toxicities, high costs, extended treatment times, serious adverse side effects, and the degree of clinical resistance.²¹⁻²³

Recognizing the pharmacological potential of chalcones already reported in the literature with regard to their antileishmanial activity, and in view of difficulties in adherence and the high toxicity of the drugs currently available for leishmaniasis treatment, the need to study new therapeutic alternatives is evident. The aim of this study was to investigate possible pharmacological activities of four new chalcones *in silico*, their leishmanicidal potential *in vitro*, and evaluate potential mechanisms of action through molecular docking.

Experimental

Test products

The synthesis of new chalcones was conducted in the Organic Chemistry Laboratory of the Post-graduate Program in Natural Products and Bioactive Synthetics at the Federal University of Paraíba (UFPB).

Synthesis was carried out through separate methylation, ethylation, and allylation of 4-hydroxybenzaldehyde, with subsequent Claisen-Schmidt condensation, which respectively yielded the first 3 chalcones. The fourth chalcone resulted from bromination on vanillin, followed by ethylation, and aldol condensation (Supplementary Information section).²⁴

In silico study-activity spectra prediction (PASS and MolPredictX)

To predict the biological activity of the structures, the four compounds were submitted to the evaluation of biological activity using two online programs.

The program PASS filter²⁵ provides quantitative

structure reactivity relationships through decomposition of chemical structures into 2D and/or 3D descriptors, with consequent production of models obtained from bioactive ligands. Through analysis, it is possible to predict the estimated activity spectrum of a compound as probable activity (Pa) and probable inactivity (Pi). The values of Pa and Pi range from 0.000 to 1.000, and a compound can be said to be experimentally active when $Pa > Pi$. When $Pa > 0.7$, the probability of experimental pharmacological activity is said to be high, values of $0.5 < Pa < 0.7$ indicate an average probability of experimental pharmacological activity, and if $Pa < 0.5$, the chance of having experimental pharmacological activity is lower, but it can still present a chance of finding a new compound.²⁶

MolPredictX²⁷ is an innovative and freely accessible web interface for predicting the biological activity of query molecules. Utilizing in-house quantitative structure-activity relationships (QSAR) models, MolPredictX provides 27 qualitative predictions (active or inactive) and quantitative probabilities for bioactivity, including against parasitic organisms such as *Trypanosoma* and *Leishmania*.²⁸ Specifically, activity against *Leishmania braziliensis* can be evaluated using a machine learning model developed by Maia *et al.*²⁹ According to this model, a structure is classified as active when its relationship between binding free energies and biological activities (pIC_{50}) value exceeds 4.5. MolPredictX also offers quantitative probability values for activity based on the random forest algorithm utilized in constructing the model.²⁹

Parasite culture

Promastigote forms of *L. braziliensis* (MHOM/BR88/BA-3456) were cultured in Schneider's medium (Sigma-Aldrich, Saint Louis, Missouri, USA) containing 10% fetal bovine serum (FBS, GIBCO, Thermo Fisher Scientific, Waltham, MA USA), 50 $\mu\text{g mL}^{-1}$ gentamicin (Life, Carlsbad, CA), pH 7.2, and incubated at 26 °C. The parasites were counted daily in a Neubauer chamber for five days. When they reached the stationary growth phase, new *in vitro* passages of the parasites were performed.³⁰

Cytotoxicity test on macrophages *in vitro*

Murine macrophages of the J774 strain were used to evaluate the activity of the compounds, being incubated in 96-well plates (1×10^4 cells *per well*) in Dulbecco's modified Eagle's medium (DMEM, Life Technologies, GIBCO-BRL, Gaithersburg, USA), supplemented with 10% fetal bovine serum (SIGMA) and 50 $\mu\text{g mL}^{-1}$ gentamicin (Life), and maintained for 24 h in an incubator at 37 °C, aerated

with 5% CO₂. Differing concentrations (100, 50, 25, 12.5, 6.25, and 3.125 μM) of the four compounds were tested, in triplicate, being incubated for 72 h. Subsequently, 20 μL of AlamarBlue (Invitrogen, Carlsbad, USA) were added for 6 h. Reading in a spectrophotometer (Microplate reader, Spectramax 190, Molecular Devices, Sunnyvale, California, USA) was performed at 570 and 600 nm. The results were expressed as 50% cytotoxic concentration values (CC₅₀). Gentian violet (Synth, São Paulo, SP, Brazil) was used as a positive control.

Antileishmanial activity

Promastigotes of *L. braziliensis* (1×10^6 *per well*) were grown in a 96-well plate in Schneider's medium (Sigma) supplemented with 10% fetal bovine serum (FBS; GIBCO) and 50 $\mu\text{g mL}^{-1}$ gentamicin (Life) and subjected to treatment with differing concentrations (100, 50, 25, 12.5, 6.25, and 3.125 μM) of the four compounds. The parasites were incubated for 72 h at 26 °C. Then, 20 μL well of AlamarBlue (Invitrogen) was added for 24 h, and reading was performed in a spectrophotometer at 570 and 600 nm. The percentage of axenic culture inhibition was determined based on the untreated control.

Selectivity index (SI) evaluation

The selectivity index (SI) was calculated using the ratio between the CC₅₀ value obtained for the macrophages and the inhibitory concentration (IC₅₀) value obtained in promastigotes treated with the molecules under study. The SI is used to determine how much more active the tested molecule is against *Leishmania* than toxic for the macrophage, indicating greater selectivity for the parasite without causing damage to the viability of mammalian cells. The SI should be greater than one (> 1).³¹

In vitro infection of macrophages and treatment with FERAI (chalcone 4)

Murine J774 macrophages were cultured in 24-well plates at a concentration of 5×10^5 with round coverslips added to the wells beforehand and infected with *L. braziliensis* in stationary phase at a ratio of 10 parasites *per* macrophage. After washing with DMEM medium, different concentrations of FERAI (20, 10, 5, and 2.5 μM), were added to the wells. Amphotericin B (AB, 5 μM) was used as a positive control. After 24 h, the cells were fixed in methanol and stained using Giemsa (Dinâmica, Química Contemporânea Ltda, SP, Brazil). The percentage of infected macrophages

and the number of amastigotes per macrophage was determined by counting 100 cells *per well*.

Evaluation of reactive oxygen species (ROS) production

L. braziliensis promastigotes (2×10^6 *per well*) were grown in a 24-well plate in Schneider's medium, supplemented with 10% fetal bovine serum, 50 $\mu\text{g mL}^{-1}$ gentamicin, and then treated with FERAI (5 to 30 μM). The parasites were incubated for 4 h at 26 °C. Subsequently, 6 μL of 2',7'-dichlorodihydrofluorescein diacetate (H₂DCFDA) (10 mM) (Invitrogen, Eugene, USA) was added to each well, being then kept for 30 min in the absence of light. Data acquisition was performed in a FACSCalibur flow cytometer (Becton Dickinson, Franklin Lakes, NJ, USA) and analyzed in FlowJo_v10.6.1.³²

Protein sequence alignment

Three proteins fundamental to the life maintenance of *Leishmania* species were used in the study: dihydroorotate dehydrogenase, trypanothione-reductase and UDP-glucose pyrophosphorylase. Since these proteins do not have 3D structures in the Protein Data Bank,³³ the corresponding sequences were obtained from the GenBank database.³⁴ A global alignment was performed using the sequence of a protein with a known three-dimensional structure and the web tool Clustal Omega,³⁵ which aligns protein sequences. The alignment facilitated investigation of the active site, determination of similarity, and shared identity between the proteins.³⁶

Homology modeling

Target sequences were obtained as amino acid sequences in FASTA format and were imported into the SWISS-MODEL website.^{37,38} Quality was predicted for each identified template using alignment resources such as ProMod3, QMEAN and GMQE. The stereo chemical quality of the templates was evaluated using

the PSVS (protein structure validation software suite)³⁹ web server and PROCHECK.⁴⁰ PROCHECK generates a Ramachandran plot,⁴¹ for allowed and disallowed regions of the main amino acid chain.

Molecular docking

Molecular docking was used to investigate the mechanism of action of the compound presenting more promise in the previous tests (ChS₄), and the binding affinity of the compound to the enzymes selected in the study, was used to elucidate a possible route contributing to the leishmanicidal effect. For this, screening with several proteins involved in these effects was performed. The 3D structures of the enzymes that served as templates for the elaborated models were obtained from the PDB.³⁵ The proteins selected and detailed information about them are presented in Table 1.

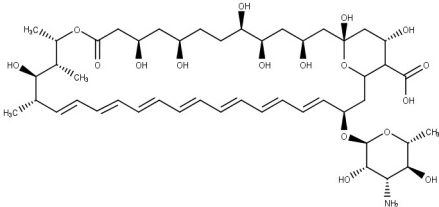
Molegro Virtual Docker v. 6.0.1 (MVD)⁴² software was used with its predefined parameters. The complexed ligand was used to define the active site. The compounds were then imported to analyze the stability of the system through interactions identified with the active site of the enzyme, taking the MolDock Score energy value as reference.⁴³

The MolDock SE (Simplex Evolution) algorithm was used with the following parameters: a total of 10 runs with a maximum of 1,500 iterations a population of 50 individuals, 2,000 minimization steps for each flexible residue, and 2,000 global minimization steps *per run*. The MolDock Score function (GRID) was used to calculate the fitting energy values. The GRID was set to 0.3 Å, and the search sphere radius was set to 15 Å. Internal electrostatic interactions, internal hydrogen bonds, and sp²-sp² twists were evaluated for ligand energy analysis.

Molecular dynamics simulations

Molecular dynamics (MD) simulations were performed to estimate the flexibility of interactions between proteins and ligands, using the GROMACS 5.0 software

Table 1. Information on the proteins selected in the study

Protein	PDB ID/homology	Positive control
Dihydroorotate dehydrogenase Trypanothione reductase UDP-glucose pyrophosphorylase	homology	 amphotericin B

(European Union Horizon 2020 Program, Sweden).^{44,45} Protein and ligand topologies were also prepared using GROMOS96 54a7 force field, and the MD simulation was performed using the point charge SPC water model, extended in a cubic box.⁴⁶ The system was neutralized by the addition of Cl⁻ and Na⁺ ions and minimized to remove poor contacts between complex molecules and the solvent. The system was also balanced at 300 K, using the 100 ps V-rescale algorithm, represented by NVT (constant number of particles, volume, and temperature), followed by equilibration pressure at 1 atm. using the Parrinello-Rahman algorithm as the NPT (particle constant pressure and temperature), up to 100 ps. MD simulations were performed in 5,000,000 steps, at 10 ns. To determine the flexibility of the structure and whether the complex was stable near the experimental structure, the root mean square deviation (RMSD) values of all C α atoms were calculated relative to the initial structures. Root mean square fluctuation (RMSF) values were also analyzed to verify the roles played by residues close to the receptor binding site. RMSD and RMSF plots were generated in Grace software and protein and ligands were visualized in UCSF Chimera.⁴⁷⁻⁵⁰

Statistical analysis

The numerical values shown in the pharmacological activity tables correspond to means \pm mean standard error (SEM), from triplicates of each experiment. Significance in the differences between the groups was evaluated using the one-way analysis of variance (ANOVA) test for analysis of variance, and the Newman Keuls multiple comparison post-test for the sample group.⁵¹

Results

PASS filter and MolPredictX predictions

The *in silico* evaluation aimed at predicting the biological activities of compounds (**1-4**) based on

their structural formulas (in SMILES format). The PASS filter and MolPredictX tools were utilized. The PASS filter indicated that all four chalcones possess antileishmanial activity, being identified among the 15 activities most likely to be exhibited by these substances (see Supplementary Information section). Further, MolPredictX,^{27,28} a freely accessible web tool developed at the Laboratory of Cheminformatics of UFPB was employed to predict the potential activity of the chalcones against *Leishmania braziliensis*. The results indicated that all four structures are active, with a probability of activity equal to 0.8 (Table 2).

Considering that the studies performed provide only a prediction of the probable, we sought other approaches that might help in the choice of biological activity to be researched. A literature investigation was therefore conducted for the years 2017 to 2021 in the SciELO, PubMed, Medline, LILACS and ScienceDirect databases, using the corresponding chemical class descriptors “flavonoids” OR “chalcones”, and noting relationships for the selected activities of each compound associated with the pharmacological activity to be researched.

Inclusion criteria included articles that related each chemical class with at least one of the 15 selected pharmacological activities, and which produced promising activity on the targets. The articles were required to be published within the latest five years, and articles that did not demonstrate potentially auspicious activity were excluded.

The results revealed that antileishmanial activity is one of the biological activities most associated with flavonoids (and against the most diverse existing species). A number of studies have reported leishmanicidal activity for compounds of this class, such as: fisetin, a polyphenolic flavonoid, which has potent activity against *Leishmania* spp. in *in vitro* tests;⁵² purified dimeric flavonoids from *Arrabidaea brachypoda* with *in vitro* activity against promastigotes and amastigotes forms of *L. amazonensis*;⁵³ flavonoids isolated from *Polygonum salicifolium* with leishmanicidal *in vitro* activity against *L. mexicana*;⁵⁴ and rusflavone, a

Table 2. Prediction of chalcone biological activity in PASS filter and MolPredictX

	PASS Filter		MolPredictX	
	Antiprotozoal (<i>Leishmania</i>)		<i>Leishmania braziliensis</i>	
	Pa	Pi	Pa	Pi
Chalcone 1	0.704	0.009	0.80	0.20
Chalcone 2	0.649	0.011	0.80	0.20
Chalcone 3	0.78	0.005	0.80	0.20
Chalcone 4	0.753	0.007	0.80	0.20

Pa: probability to be active; Pi: probability to be inactive.

biflavonoid isolated from the pollen of *Attalea funifera* presenting activity against promastigote and amastigote forms of *L. amazonensis* through a mechanism that involves the production of reactive oxygen species, mitochondrial dysfunction, and membrane disruption in the parasites.⁵⁵

For chalcones, scientific research can also be found reporting broad leishmanicidal activity against various *Leishmania* species.⁵⁶ The studies of Nardella *et al.*⁵⁷ indicate that regardless of the assay performed, whether *in vitro* or *in vivo*, the most active compounds against *Leishmania* spp. belong to the chalcone, biflavone, and aurone classes. Phytochemical evaluation of the chalcones, 2',4'-dimethoxy-6'-hydroxychalcona and 2',5'-dimethoxy-4',6'-dihydroxychalcona has revealed promising antileishmania activity against *L. mexicana*, with no toxicity in human cell line tests.⁵⁷ The leishmanicidal activity of 31 synthetic chalcones was analyzed *in vitro*, using promastigotes and amastigotes of *L. donovani*, *L. tropica*, *L. major*, and *L. infantum*, and the results indicated that 16 of the compounds were active, while presenting high selectivity, and low toxicity against mammalian cells.⁵⁸

It was decided to initially proceed with *in vitro* antileishmanial activity tests (for screening) followed by more complex studies.

Cytotoxicity and antileishmanial activity

Cytotoxicity evaluation (CC_{50}) was performed in J774 murine macrophages, and the results for each compound were compared to gentian violet ($CC_{50} = 0.7 \pm 0.09 \mu\text{M}$), a known cytotoxic drug, or amphotericin B (AB), the antileishmanial reference drug. All chalcones exhibited $CC_{50} > 50$, being several times less cytotoxic than amphotericin B ($CC_{50} = 3.6 \mu\text{M}$) (Table 3).

Antileishmanial activity in an axenic culture was used to calculate the EC_{50} value and evaluate the activity

of the compounds against *L. braziliensis* promastigotes. Compounds **1-3** did not present promising inhibitory potency, obtaining EC_{50} values above $50 \mu\text{M}$, as compared to AB used as a positive control ($EC_{50} = 0.32 \pm 0.01 \mu\text{M}$). However, FERAI presented potent activity inhibiting the growth of *L. braziliensis* promastigotes, with an EC_{50} value of $9.75 \pm 1.7 \mu\text{M}$ (Table 3). In view of these results, we decided to continue with the chalcone **4** tests, now called "FERAI", because it proved to be the most promising compound.

In addition, FERAI demonstrated significant activity against amastigote forms of *L. braziliensis* with an EC_{50} value of $10.13 \pm 1.7 \mu\text{M}$. AB presented an EC_{50} value of $0.7 \pm 0.004 \mu\text{M}$ for this same parasite. The SI, as calculated from the ratio between the CC_{50} and EC_{50} values for FERAI was 6.8 times more selective (SI) for promastigotes, and 6.6 times more potent for *L. braziliensis* amastigotes than for mammalian cells. AB was respectively 11.25 and 5.14 times more selective (SI) (Table 3). Thus, FERAI presented a higher selectivity index for amastigotes than AB, the reference drug.

FERAI also reduced the infection of macrophages by *L. braziliensis*. Murine macrophages of the J774 strain were infected with *L. braziliensis* amastigotes and treated with various concentrations of FERAI, which caused a concentration-dependent reduction in the percentage of macrophages infected, and the number of intracellular parasites *per* 100 macrophages when compared to the control group. As expected, AB also decreased the number of infected macrophages and the number of amastigotes *per* 100 cells (Figure 1).

FERAI significantly alters the production of ROS in *L. braziliensis* promastigotes

ROS levels were measured using the permeable dye H_2DCFDA , aiming to investigate whether the leishmanicidal effect of FERAI in *L. braziliensis* promastigotes is due to

Table 3. Cytotoxicity evaluation (CC_{50}), half maximal effective concentration for 50% of promastigotes and intracellular parasites forms (EC_{50}), and selectivity index (SI) of chalcones

Compound	$CC_{50} \pm \text{S.D.}$ M ϕ J774 / μM	$EC_{50} \pm \text{SD}$ promastigotes <i>L. braziliensis</i> / μM	SI promastigotes <i>L. braziliensis</i>	EC_{50} amastigotes <i>L. braziliensis</i> / μM	SI amastigotes <i>L. braziliensis</i>
1	> 50	> 50	–	–	–
2	> 50	> 50	–	–	–
3	> 50	> 50	–	–	–
4 (FERAI)	> 50	9.75 ± 1.7	6.8	10.13 ± 1.7	6.6
Amphotericin B (AB)	3.6 ± 0.50	0.32 ± 0.01	11.25	0.7 ± 0.004	5.14
Gentian violet	0.7 ± 0.09	–	–	–	–

Values calculated from two independent experiments. SD: standard deviation.

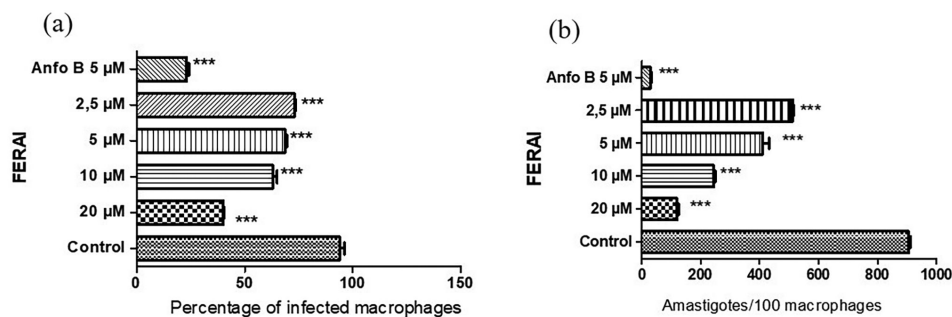


Figure 1. Effect of FERAI against intracellular parasites of *L. braziliensis*. Macrophages were infected by *L. braziliensis* (10:1) and treated with four different concentrations of FERAI 1:2, (2.5 to 20 µM) and amphotericin B (5 µM) for 24 h. The percentage of infected macrophages (a) and the number of intracellular parasites *per* 100 macrophages (b) were determined after 24 h of treatment.

ROS production. FERAI induced ROS production in promastigotes (with increased ROS levels) noted especially at the highest concentrations used: 10 µM (56.33%), 20 µM (61.76%) and 30 µM (67.13%) compared to the untreated control. Hydrogen peroxide (H₂O₂) was used as a positive control (Figure 2).

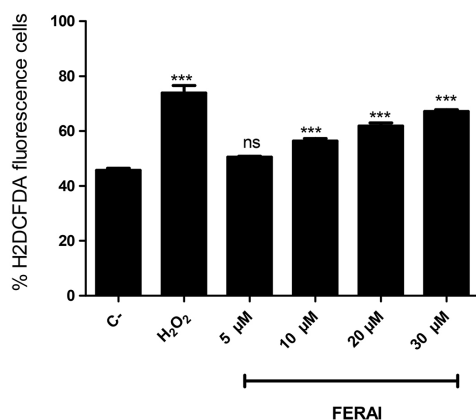


Figure 2. Evaluation of intracellular ROS levels in *L. braziliensis* promastigotes. Evaluation of intracellular ROS levels induced using FERAI at different concentrations (5 to 30 µM) for 24 h and incubated with H₂DCFDA probe for 30 min. ****p* < 0.001 and ns = not significant compared to untreated control.

The average values of the FERAI samples, the positive and negative controls, and the standard deviation were also calculated (Table 4).

Protein sequence alignment

Shared amino acids between target and template protein sequences were investigated. The results revealed that trypanothione reductase (*L. braziliensis*) possesses 84.01% identity with trypanothione reductase from *L. infantum* (PDB: 3JK6). While dihydroorotate dehydrogenase for *L. braziliensis* possesses 84.66% identity with dihydroorotate dehydrogenase from *L. major* (PDB: 6EBS) (see Supplementary Information section).

Table 4. Evaluation of intracellular ROS levels in *L. braziliensis* promastigotes (mean and standard deviation of positive control and untreated control samples)

Sample	ROS / %	
	Mean	Pattern deviation
Negative control	45.66	± 1.14
H ₂ O ₂	73.9	± 3.74
FERAI 5 µM	50.50	± 0.43
FERAI 10 µM	56.33	± 1.27
FERAI 20 µM	61.76	± 1.58
FERAI 30 µM	67.13	± 0.59

ROS: reactive oxygen species.

UDP-glycosyl pyrophosphorylase from *L. braziliensis*, presented 96.93% identity with UDP-glycosyl pyrophosphorylase from *L. major* (PDB: 2OEF).

Homology modeling

The enzyme models for dihydroorotate dehydrogenase, trypanothione reductase and UDP-glycosyl pyrophosphorylase were generated using the homology modeling method. The reliability of the models was assessed using the Ramachandran plot, which represents all possible combinations of dihedral angles Ψ (psi) versus φ (phi) for each amino acid in a protein except glycine, which has no side chains. The models are considered reliable when more than 90% of the amino acids are present in the allowed and/or favored regions (colored regions of the plot). Blank regions represent discrepant values, with poor contacts. The dihydroorotate dehydrogenase model presented 91.8% amino acids in the favored regions and 8.2% in allowed regions. The trypanothione reductase model presented 91.6% of amino acids in the favored regions and 8% in allowed regions. Finally, the UDP-glycosyl pyrophosphorylase model percentages corresponded to 93.5% of amino acids in the favored regions and 6.3% in the allowed regions. Considering the results, the homology models were considered reliable (Figure 3).

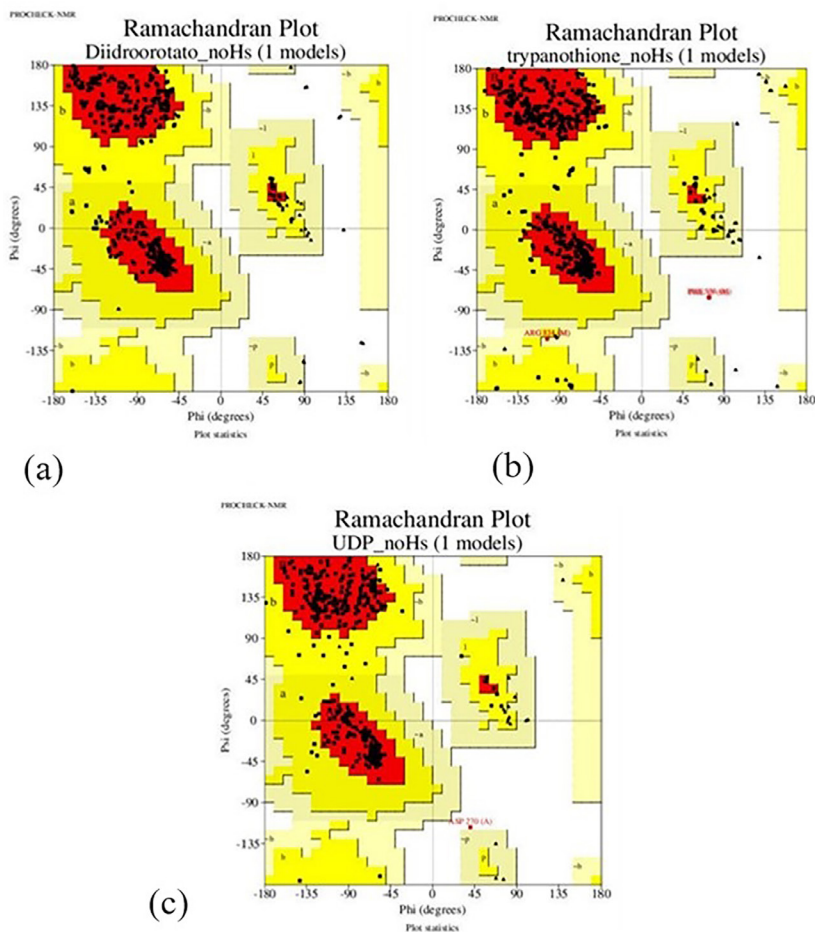


Figure 3. Ramachandran plots of the homology modeling generated for the enzymes: dihydroorotate dehydrogenase (a), trypanothione reductase (b) and UDP-glucose pyrophosphorylase (c).

Molecular docking

Chalcone **4** (FERAI) was subjected to screening using molecular docking on 3 proteins. The docking results were generated using two scoring functions, the Moldock Score and the Rerank Score. In most of the scoring functions, the more negative values indicated better predictions. The protein in which the compound obtained binding energy values higher or close to the standard drug in at least one scoring function was considered active (Table 5).

Of the three proteins analyzed, chalcone **4** obtained negative energies for all the enzymes under study. Moreover, it obtained better results with dihydroorotate dehydrogenase

and trypanothione reductase, and it obtained values close to or higher than the values of MolDockscore and Rerankscore as compared to the controls. Chalcone **4** exhibited greater potency against proteins dihydroorotate dehydrogenase and trypanothione reductase, with respective binding affinity values of -132.276 and -151.281 kcal mol⁻¹.

We analyzed in detail the interactions and bonds formed with the test compound and the dihydroorotate dehydrogenase and trypanothione reductase proteins.

The test compound (chalcone **4**) was capable of forming four hydrophobic interactions with the amino acids Val 22, Ala 19, Cys 249, and Met 70; also forming seven hydrogen bonds with the amino acids Lys 44, Gly 21,

Table 5. Binding energy values analyzed in the three selected proteins in the study

Protein	Chalcone 4 (FERAI)		Amphotericin B-positive control	
	Moldock score	Rerank score	Moldock score	Rerank score
Dihydroorotate dehydrogenase	-132.276	-95.1107	-43.403	1141.65
Trypanothione reductase	-151.281	-317.774	-102.191	-282.763
UDP-glucose pyrophosphorylase	-56.8384	-39.1568	-146.389	-64.8544

Gly 272, Gly 223, Cys 249, Asn 195, and Lys 44 at the active site of the protein dihydroorotate dehydrogenase (Figure 4). Amphotericin B formed seven hydrogen bonds with residues Ser 45, Asn 128, Lys 165, Gly 250, Ile 194, Thr 273, Ala 20, and Met 20; six hydrophobic interactions with residues Pro 73, Glu 29, Met 20, Met 23, Ala 19, and Cys 249; and twelve steric interactions with residues Met 20, Glu 29, Met 23, Val 12, Gln 276, Tyr 59, Ser 198, Gly 122, Asn 199, Ser 98, Lys 44, and Lys 165. Coincidences occurred between the positive control and the test compound at the hydrophobic interaction of residue Cys 249.

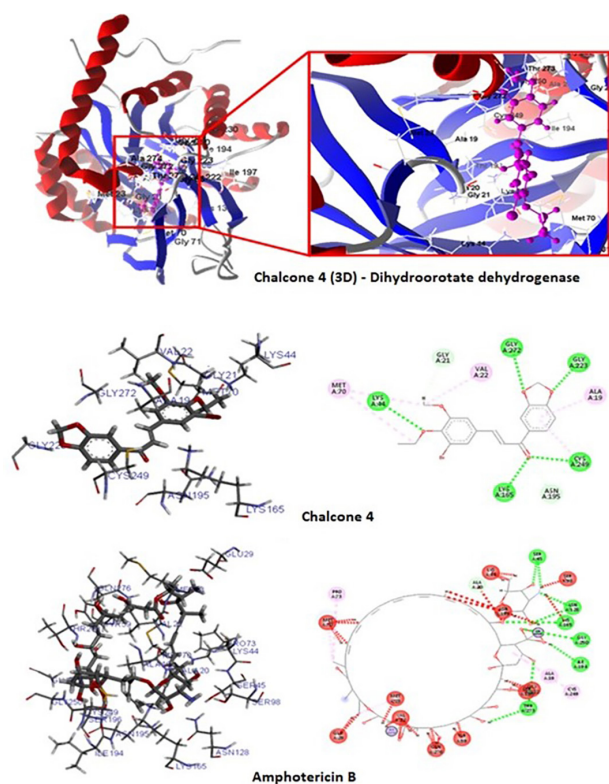


Figure 4. 2D and 3D interactions between chalcone 4, amphotericin B and the protein dihydroorotate dehydrogenase.

For trypanothione reductase, the test compound established six hydrophobic interactions the active site with Thr 160, Ala 398, Ala 159, Val 36, Leu 10, and Val 34; and five hydrogen interactions, which corresponded to Gly 161, Ser 14, Asp 35, and Gly 15 (Figure 5). Amphotericin B, on the other hand, presented five hydrogen bonds with residues Gly 49, Thr 51, Cys 57, Tyr 198, and Arg; and ten steric interactions with residues Pro 336, Ile 339, Val 53, Cys 52, Ser 14, Asp 327, Met 333, Thr 51, Tyr 198, and Cys 57. A hydrophobic interaction with amino acid Val 53 was also recorded. For this enzyme no similar interactions occurred between the test compound and the positive control.

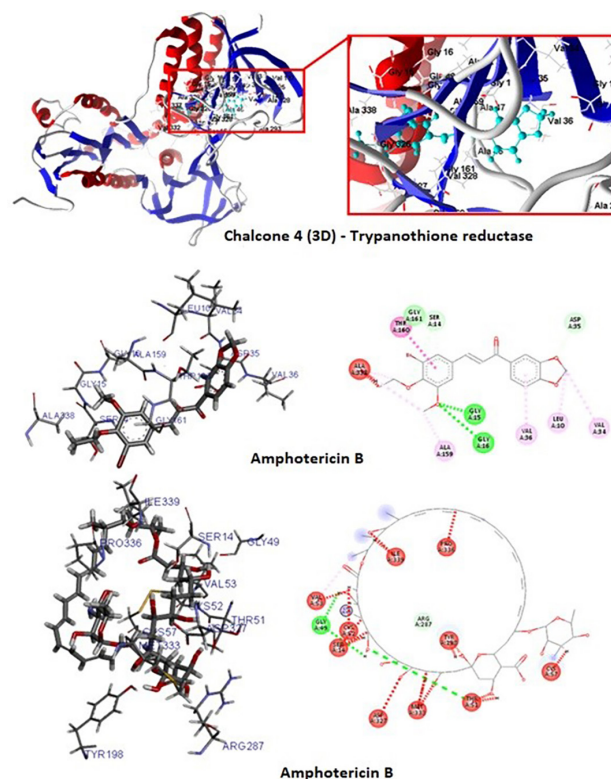


Figure 5. 2D and 3D interactions between chalcone 4, amphotericin B, and trypanothione reductase.

Trypanothione reductase

For trypanothione reductase, analysis of the RMSD metric of the protein (Figure 6a) revealed that the complexes related to the protein (black line) and compound 4 (FERAI) (red line) presented greater stability than the control drug amphotericin B (green line); presenting much lower RMSD values. Various fluctuations were also observed in the complex referring to amphotericin B. For FERA1, it was observed that after a period of 15 ns the RMSD values remained constant at 0.4 nm, remaining without change throughout the total simulation time; denoting high stability. The protein complex presented fluctuations between 30 and 50 ns with RMSD values of up to 0.55 nm, which returned to 0.4 nm after 55 ns. The control drug amphotericin B was significantly more unstable after 50 ns, as values reached 0.6 nm and remained so until the total time of 100 ns.

When analyzing the stability of the ligands in the presence of solvents (Figure 6b), it was verified that the result corroborated the RMSD results, since FERA1 (black line) presented lower RMSD values than the control drug amphotericin B (red line), which was significantly more unstable.

To better understand the flexibility of residues and amino acids contributing to the conformational change in the trypanothione reductase enzyme, the RMSF of each

amino acid in the protein were calculated. Residuals with high RMSF values reflect more flexibility and low RMSF values suggest less flexibility. Considering that amino acids with fluctuations above 0.3 nm contribute to the flexibility of the channel structure, residues in positions 1-2, 79, 81-87, 89, 305, 355, 458-462, and 480-483 (Figure 7a) contributed to the conformational change and flexibility of the complexed protein.

The Coulomb and Lennard-Jones interaction energies (Table 6) of the protein-ligand complexes were calculated. FERAI demonstrated greater interaction stability with the active site due to a greater influence of electrostatic and hydrogen interactions. According to Lennard-Jones metrics, the control amphotericin B demonstrated greater stability than FERAI.

Table 6. Coulomb and Lennard-Jones interaction energy values

	Energy / (KJ mol ⁻¹)	
	Compound 4 (FERAI)	Amphotericin B
Coulomb (C)	-172.534	-80.377
Lennard-Jones (LJ)	-171.133	-209.129

Dihydroorotate dehydrogenase

For dihydroorotate dehydrogenase, according to the protein RMSD metric (Figure 6c), the greater instability

observed in the three complexes analyzed reflected the occurrence of a greater number of fluctuations. The control amphotericin B (green line) presented the greatest stability, with lower RMSD values. FERAI (red line) presented RMSD values of 0.5 nm and fluctuations during the periods at 50 and 90 ns.

When analyzing the stability of the ligands in the presence of solvents (Figure 6d), it was found that FERAI (black line) was significantly more unstable than amphotericin B (red line). FERAI presented RMSD values of 0.4 nm, while amphotericin B presented values of 0.18 nm.

To assess the flexibility of the residues and amino acids that contribute to the conformational change in dihydroorotate dehydrogenase, the RMSF of each amino acid in the protein were calculated. It was observed that residues at positions 201, 204-209, 216, and 310-312 contribute to the conformational change of the protein complexed with FERAI (Figure 7b).

The Coulomb and Lennard-Jones interaction energies (Table 7) of the protein-ligand complexes were calculated. FERAI demonstrated greater interaction stability with the active site through Lennard-Jones energy calculations, which denotes a greater influence of van der Waals interactions. According to the Coulomb metrics, the amphotericin B control demonstrated greater stability than FERAI.

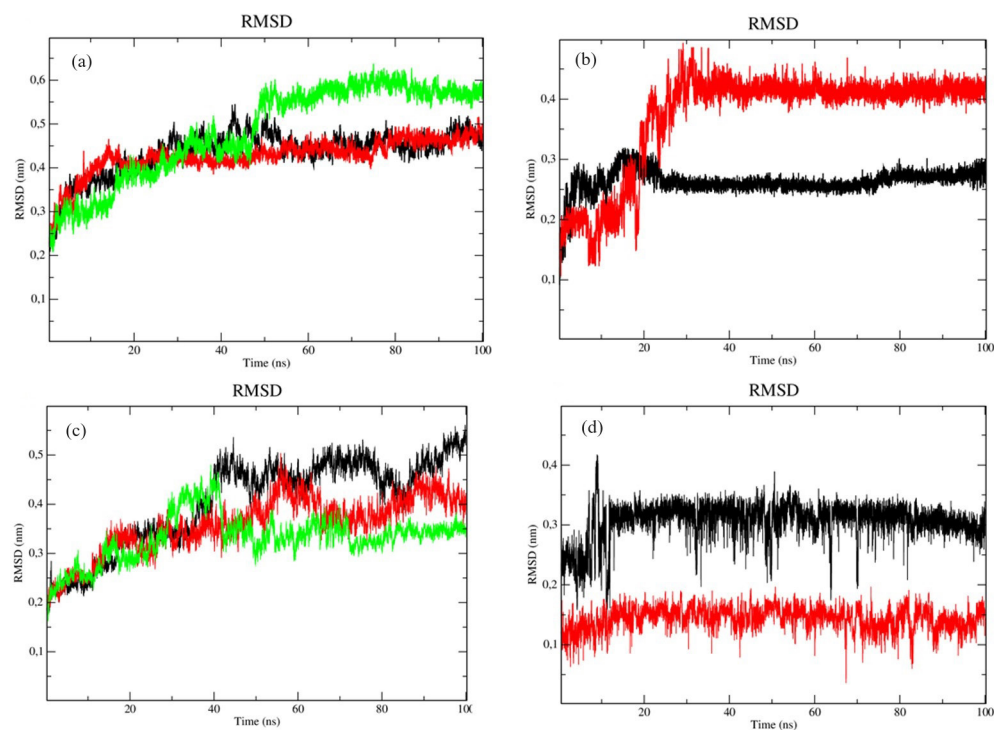


Figure 6. RMSD of C α atoms. (a) Trypanothione reductase (black), complexed with FERAI (red) and amphotericin B (green). (b) FERAI (black line), and amphotericin B (red line). (c) dihydroorotate dehydrogenase (black), complexed with FERAI (red) and amphotericin B (green). (d) FERAI (black line), and amphotericin B (red line).

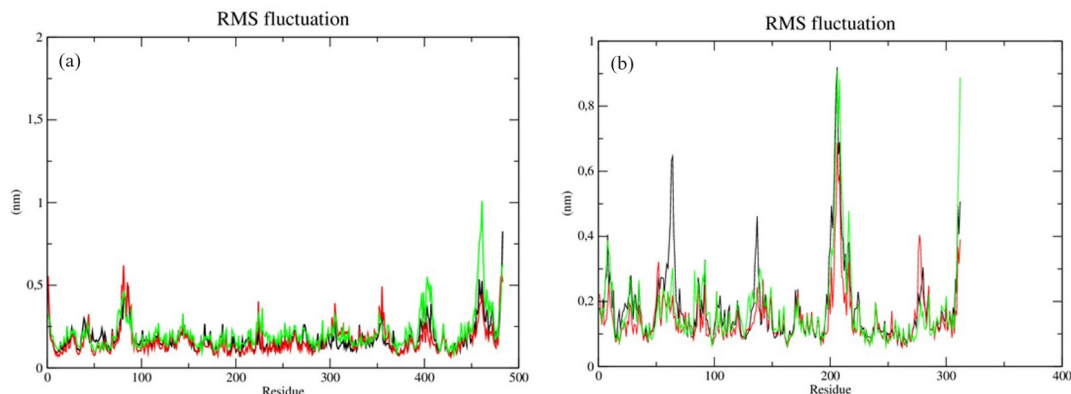


Figure 7. RMSF of atoms. (a) Enzyme (black line) complexed to FERAI (red line) and amphotericin B (green line). (b) Enzyme dihydroorotate dehydrogenase (black line) complexed to FERAI (red line) and amphotericin B (green line).

Table 7. Coulomb and Lennard-Jones interaction energy values

	Energy / (KJ mol ⁻¹)	
	Compound 4 (FERAI)	Amphotericin B
Coulomb (C)	-58.6761	-83.475
Lennard-Jones (LJ)	-158.865	-126.96

Discussion

Through the use of computer simulations, computational chemistry and bioinformatics have taken an innovative role in directing studies and drug planning.⁵⁹ In this context, the use of *in silico* models has evolved with remarkable progress in many areas such as correlation, prediction, simplification, automation, among other expressive aspects.⁶⁰

Development of new drugs is a complex process that requires both time and financial resources. Computer-aided studies aim to create new approaches that boost research and provide avenues for further testing. Virtual screening for identification and optimization of other testing methodologies is an advantage of these studies, as it is possible to predict pharmacological activity for a specific molecule, quantifying activity and inactivity with a probability score.^{61,62}

As an initial screening regarding pharmacological activity, it was possible to observe in both the PASS and MolPredictX studies that the four chalcones presented similar results for the 15 activities with higher probabilities of occurrence in both. The fact that the four substances belong to the same class could explain the occurrence of similar results among them, taking into account that the tests work using decomposition of the molecular structure into 2D and 3D descriptors which they are expected to have in common.

Based on the literature,⁶³⁻⁶⁵ and seeking to elect the pharmacological activity most associated with chalcones,

it was observed that antileishmania activity has been well researched and that these substances present promising activity with regard to potency and efficacy against various species.

A number of studies have reported leishmanicidal activity for this class of compounds, such as fisetin, a polyphenolic flavonoid, which has potent *in vitro* action against *Leishmania* spp.,⁵² purified dimeric flavonoids from *Arrabidaea brachypoda* with *in vitro* action against promastigotes and amastigotes forms of *L. amazonensis*,⁵³ flavonoids isolated from *Polygonum salicifolium* with *in vitro* leishmanicidal activity against *L. mexicana*,⁵⁴ and rusflavone, a biflavonoid isolated from the pollen of *Attalea funifera*, which has been shown to act against the promastigote and amastigote forms of *L. amazonensis*, through a mechanism that involves the production of ROS, mitochondrial dysfunction, and membrane disruption in the parasites.⁵⁵

As for chalcones, scientific research can also be found indicating broad leishmanicidal activity against various species of the genus *Leishmania*.⁵⁶ The studies of Nardella *et al.*⁵⁷ indicated that regardless of the assay performed, whether *in vitro* or *in vivo*, the most active compounds against *Leishmania* spp. belong to the chalcone, biflavone, and aurone classes. The phytochemical evaluations of the chalcones, 2',4'-dimethoxy-6'-hydroxychalcone and 2',5'-dimethoxy-4',6'-dihydroxychalcone presented promising antileishmania activity against *L. mexicana*, with no toxicity in tests with a human cell line.⁴⁹ The leishmanicidal activity of 31 synthetic chalcones was analyzed *in vitro* using promastigotes and amastigotes of *L. donovani*, *L. tropica*, *L. major*, and *L. infantum*. The results indicated that 16 of the compounds were active against the strains, showing high selectivity and low toxicity against mammalian cells.⁵² In view of this, it was decided to continue our research in this area.

Cytotoxicity assays at the beginning of studies with natural products are among the principal *in vitro* tests used.

They predict toxicity, and provide a means for evaluation, safety screening, and classification of compounds. The monitoring of cell response within these assays provides reliable results and can serve as a basis for measuring other parameters such as cell viability and SI.^{66,67}

When compared using gentian violet, the cytotoxicity test results for murine macrophages demonstrated the low cytotoxicity of the four chalcones ($CC_{50} = 0.6 \pm 0.01 \mu\text{M}$), with CC_{50} values above $50 \mu\text{M}$. These were encouraging results, as it is essential that new antileishmanial drug candidates present reduced cytotoxicity to overcome the disadvantages of drugs currently used in therapy.

Another study⁶⁸ investigating the effects of twenty brominated chalcones against four cancer cell lines reported similar results, the tested substances exhibited lower cytotoxicity for non-malignant gastric epithelial cells than for diseased ones, demonstrating selectivity. Researchers investigated the *in vitro* cytotoxicity of ten chalcones against the HeLa cell line through the thiazoyl blue tetrazolium bromide (MTT) viability assay and SI calculation, and the results revealed the low cytotoxicity of these substances in this cell type.⁶⁹

It was observed during the axenic culture analysis for antileishmanial activity that chalcones **1**, **2**, and **3** did not present promising inhibitory potency (IC_{50}). However, chalcone **4**, which was the most potent in inhibiting the growth of *L. braziliensis*, presented low cytotoxicity when compared to AB, being therefore a promising candidate for future tests.

A number of studies^{61,65,70} have reported chalcones with potent antileishmanial activity against *L. braziliensis*. Two synthetic chalcones were evaluated *in vitro* against *L. braziliensis* promastigotes for inhibitory activity and cytotoxicity against macrophages. The IC_{50} and CC_{50} results were respectively, 1.38 ± 1.09 ; $6.36 \pm 2.04 \mu\text{M}$, and 13.49 ± 3.13 ; $199.43 \pm 4.11 \mu\text{M}$, and both presented effects against *L. braziliensis* promastigotes, with low toxicity to mammalian cells.⁶³

Similar results were found in a study involving three methoxy chalcones, which presented significant *in vitro* antileishmanial activity against *L. braziliensis* promastigotes ($IC_{50} = 2.7, 3.9, \text{ and } 4.6 \mu\text{M}$), with more potent activity than the control drug pentamidine ($IC_{50} = 6.0 \mu\text{M}$).⁷¹

The potential for FERAI activity to involve increased ROS levels in *L. braziliensis* promastigotes was also investigated. The results indicated an increase in ROS levels, at concentrations of $10 \mu\text{M}$ (56.33%), $20 \mu\text{M}$ (61.76%), and $30 \mu\text{M}$ (67.13%) compared to the untreated control. Similar results were found by Santiago-Silva *et al.*,⁷² who evaluated the production of ROS by chalcone ((*E*)-1-(4,8-dimethoxynaphthalen-1-yl)-3-(4-nitrophenyl)

prop-2-en-1-one), which induced several morphological and ultrastructural changes in free promastigotes, including loss of plasma membrane integrity, and an increase in ROS.

Given our results, it was hypothesized that the addition of bromine to compound **4** optimized its antileishmanial effects. Reports in the literature⁷³ already report that brominated synthetic substances possess superior bioactive potential, and although the mechanisms that explain these results are not yet fully elucidated, one can cite possibilities. High lipophilicity and permeability through biological membranes, increased half-life, and the ability to form intermolecular bonds (attractive interactions) between the electrophilic region of the molecule containing bromine atoms and nucleophilic active sites of the biomolecule. Bromination can lead to increased therapeutic potency and research in the area of chemoinformatics can provide important contributions to elucidate its molecular interactions.⁷³ Thus, we decided to continue our studies with chalcone **4**, with tests investigating its action on *L. braziliensis* amastigotes, and evaluating its SI.

L. braziliensis is associated with both metastasis and the mucosal form of leishmaniasis, and underlies the importance of developing more effective and less toxic drugs for treatment.^{74,75} When the pharmacological activity of FERAI was evaluated against amastigotes of *L. braziliensis*, an IC_{50} value of $10.13 \pm 1.7 \mu\text{M}$ was observed. AB, a drug commercially available for the treatment of leishmaniasis, presented an IC_{50} value of $0.7 \pm 0.004 \mu\text{M}$. Although FERAI presented a higher inhibitory concentration, the result still presents promise when its low toxicity compared to AB is considered. FERAI may yet be a future drug candidate for leishmaniasis treatment since macrophages infected with *L. braziliensis* amastigotes and treated with FERAI resulted in a reduction of both the number of infected macrophages and the number of amastigotes *per* macrophage, confirming its significant activity on intracellular forms of *L. braziliensis*.

Protein sequence alignment helps to verify the similarity and identify the same protein in different species or different proteins from the same species. With this technique, it is possible to analyze conserved regions and identify common residues in the active site. In addition, it is possible to point out differences and structural similarities that can contribute to drug development. Amino acids shared between the sequences of the target and template proteins have been investigated.^{76,77}

Alignment of the *L. braziliensis* trypanothione-reductase protein sequences with trypanothione reductase from *L. infantum*; the *L. braziliensis* dihydroorotate dehydrogenase with dihydroorotate dehydrogenase from *L. major*; and *L. braziliensis* UDP-glycosyl

pyrophosphorylase with UDP-glycosyl pyrophosphorylase from *L. major*, revealed a high degree of identity and similarity, which enabled the construction of reliable homology models for these proteins.

Molecular docking, when applied to analyze natural products as candidates for new drugs, makes it possible to obtain data on mechanisms of action, molecular interactions, and substance-target binding.^{78,79} Molecular docking is a fast, low-cost and efficient technique, and is very useful for working with both natural and synthetic products, allowing reduction of material losses, and better use of the substances.^{9,80}

In the molecular docking results, chalcone **4** (FERAI) obtained negative energies for all of the enzymes under study, demonstrating interaction with all the targets. Further, FERA1 interacted more specifically with dihydroorotate dehydrogenase and trypanothione reductase, and this may reflect a certain specificity of the compound, since it presented higher energy in two specific targets.

After analyzing the potential activity of FERA1 in relation to important mechanisms for evaluating antileishmanial activity, molecular dynamics simulations were carried out to evaluate the flexibility of the enzymes and the stability of interactions in the presence of factors such as solvent, ions, pressure, and temperature. Such information is important because it complements docking results and allows us to evaluate whether the compound remains strongly bound to the studied enzymes in the presence of factors that are found in the host organism. For this analysis, the enzymes trypanothione reductase and dihydroorotate dehydrogenase were chosen since FERA1 presented greater affinity for these proteins. RMSD was calculated separately for the C α atoms of the complexed enzyme and the structures of each ligand.

Ligand stability is essential in pharmacological activity studies, as this factor, for keeping compounds bound to the active site, can be a determining factor in both potency and efficacy.^{81,82} The trypanothione reductase protein complex proved to be more stable than the dihydroorotate dehydrogenase complex, which in turn was the most unstable complex, as it presented the highest RMSD values, corresponding to 0.5 nm.

Similar to amphotericin B, FERA1 was capable of establishing strong bonds with the active site, tending to remain even in the presence of solvents, ions, and other factors. Enzyme conformational flexibility is necessary for the production of certain effects, and the evidence suggests that enzyme folding and unfolding may indicate a loss of enzyme activity that precedes any marked changes in protein conformation.⁸³ Flexibility results for the amino acid residues of trypanothione reductase revealed that

of the amino acids present in the protein, the residues in positions 1-2, 79, 81-87, 89, 305, 355, 458-462, and 480-483 favored conformational changes and protein flexibility when complexed with the compound. This may be related to the fact that the protein under study was constructed using homology modeling.

The Coulomb and Lennard-Jones interaction energy calculations for the protein-ligand complexes and compound **4** (FERAI) demonstrated stable RMSD and interaction energies which in addition to enabling interaction, flexibility and stability, suggests that compound **4** interacts at the active site of the trypanothione reductase enzyme. It was also observed that the RMSD of FERA1 did not present high stability for dihydroorotate dehydrogenase, suggesting that the compound does not interact significantly with this enzyme.

Conclusions

Based on our results, the four compounds tested did not present significant cytotoxicity compared to amphotericin B. However, of the compounds tested, FERA1 presented the highest potency against *L. braziliensis* promastigotes and amastigotes, and was also able to reduce the both percentage of *Leishmania* infected macrophages, and the number of intracellular parasites *in vitro*. The ROS test results indicated that the compound possibly acts by increasing ROS in the parasite and may be one of the mechanisms of action involved in antileishmanial activity of FERA1. Molecular docking revealed that FERA1 interacts with UDP-glycosyl pyrophosphorylase, with stronger, more potent inhibition of dihydroorotate dehydrogenase, and trypanothione reductase. Trypanothione reductase, a possible target for FERA1 in *L. braziliensis* presented more stable RMSD and Coulomb and Lennard-Jones interaction energies as well.

Supplementary Information

Supplementary information concerning the synthesis of the molecules, characterization and extra information on the protein-binding sequence of the enzymes involved in this study are available free of charge at <http://jbcs.sbq.org.br> as PDF file.

Acknowledgments

We thank the Federal University of Paraíba and its Postgraduate Program in Natural Products and Bioactive Synthetics for their institutional support, and also the Oswaldo Cruz Foundation (Fiocruz), Bahia-BR for

instrumental and technological support.

Author Contributions

Silva, G. R., Sousa, N. F., Leite, F. F. were responsible for investigation, writing original draft, validation; Santos, F. S., Acevedo, C. A. H., Grimaldi, G. B. for conceptualization, formal analysis; Soares, M. B. P., Guimarães, E. T., Rodrigues, L. C., Campana, E. H. for funding acquisition, project administration; Scotti, M. T., Mendonça, F. J. B. for resources, validation, visualization; Barbosa Filho, J. M., Guimarães, H. I. F. and Guerra, F. Q. S. for writing-review and editing.

References

- Mohammad, B.; Khurshid, A.; Sudeep, R.; Jalaluddin, M. A.; Mohd, A.; Mohammad, H. S.; Saif, K.; Mohammad, A. K.; Ivo, P.; Inho, C.; *Curr. Pharm. Des.* **2016**, *22*, 572. [Crossref]
- Raies, A. B.; Bajic, V. B.; *Comput. Mol. Sci.* **2016**, *6*, 147. [Crossref]
- Yang, X.; Wang, Y.; Byrne, R.; Schneider, G.; Yang, S.; *Chem. Rev.* **2019**, *119*, 10520. [Crossref]
- Aliper, A.; Plis, S.; Artemov, A.; Ulloa, A.; Mamoshina, P.; Zhavoronkov, A.; *Mol. Pharmaceuticals* **2016**, *13*, 2524. [Crossref]
- Gloriozova, T. A.; Dembitsky, V. M.; *Int. J. Chem. Stud.* **2018**, *6*, 832. [Link] accessed in July 2024
- Jiao, X.; Ma, Y.; Yang, Y.; Li, J.; Liang, L.; Liu, R.; Li, Z.; *Comput. Biol. Chem.* **2021**, *90*, 107402. [Crossref]
- Sakai, M.; Nagayasu, K.; Shibui, N.; Andoh, C.; Takayama, K.; Shirakawa, H.; Kaneko, S.; *Sci. Rep.* **2021**, *11*, 525. [Crossref]
- Gupta, M.; Sharma, R.; Kumar, A.; *Biol. Chem.* **2018**, *76*, 210. [Crossref]
- Zaid, N. A. M.; Sekar, M.; Bonam, S. R.; Gan, S. H.; Lum, P. T.; Begum, M. Y.; Rani, N. N. I. M.; Vaijanathappa, J.; Wu, Y. S.; Subramanian, V.; Fuloria, N. K.; Fuloria, S.; *Drug Des., Dev. Ther.* **2022**, *16*, 23. [Crossref]
- Al-Shuaeeb, R. A. A.; El-Mageed, H.; R.; A.; Ahmed, S.; Mohamed, H. S.; Hamza, Z. S.; Rafi, M. O.; Ahmad, I.; Patel, H.; *J. Biomol. Struct. Dyn.* **2023**, *41*, 23. [Crossref]
- Thayumanavan, G.; Jeyabalan, S.; Fuloria, S.; Sekar, M.; Ravi, M.; Selvaraj, L. K.; Bala, L.; Chidambaram, K.; Gan, S. H.; Rani, N. N. I. M.; Begum, M. Y.; Subramanian, V.; Sathasivam, K. V.; Meenakshi, D. U.; Fuloria, N. K.; *Molecules* **2022**, *27*, 2572. [Crossref]
- Njogu, P. M.; Guantai, E. M.; Pavadai, E.; Chibale, K.; *ACS Infectious Diseases* **2015**, *2*, 8. [Crossref]
- Ullah, A.; Munir, S.; Badshah, S. L.; Khan, N.; Gani, L.; Poulson, B. G.; Emwas, H.; Jaremko, M.; *Molecules* **2020**, *25*, 22. [Crossref]
- Moradian, N.; Hatam, G.; Hamed, A.; Pasdaran, A.; *Chem. Biol. Drug Des.* **2023**, *101*, 6. [Crossref]
- Lourenço, E. M. G.; Silva, F.; Neves, A. R.; Bonfá, I. S.; Ferreira, A. M. T.; Menezes, A. C. G.; Silva, M. C. E.; Santos, J. T.; Martines, M. A. U.; Perdomo, R. T.; Toffoli-Kadri, M. C.; Barbosa, E. G.; Sabá, S.; Beatriz, A.; Rafique, J.; Arruda, C. C. P.; Lima, D. P.; *ACS Infect. Dis.* **2023**, *9*, 2048. [Crossref]
- Chepkirui, C.; Ochieng, P. J.; Sarkar, B.; Hussain, A.; Pal, C.; Yang, J.; Coghi, P.; Akala, H. M.; Derese, S.; Ndakala, A.; Heydenreich, M.; Wong, V. K. W.; Erdélyi, M.; Yenesew, A.; *Fitoterapia* **2021**, *149*, 104796. [Crossref]
- Al-Huqail, A. A.; Bekhit, A. A.; Ullah, H.; Ayaz, M.; Mostafa, N. M.; *Agronomy* **2023**, *13*, 2765. [Crossref]
- Hernández-Rivera, J. L.; Espinoza-Hicks, J. C.; Chacón-Vargas, K. F.; Carrillo-Campos, J.; Sánchez-Torres, L. E.; Camacho-Dávila, A. A.; *Mol. Diversity* **2023**, *27*, 2073. [Crossref]
- Santos, R. F.; Silva, T.; Brito, A. C. S.; Inácio, J. D.; Ventura, B. D.; Mendes, M. A. P.; Azevedo, B. F.; Siqueira, L. M.; Almeida-Amaral, E. E.; Dutra, P. M. L.; Da-Silva, S. A. G.; *Front. Cell. Infect. Microbiol.* **2023**, *12*, 1059168. [Crossref]
- Rudrapal, M.; Khan, J.; Dukhyil, A. A. B.; Alarousy, R. M. I. I.; Attah, E. I.; Sharma, T.; Khairnar, S. J.; Bendale, A. R.; *Molecules* **2021**, *26*, 7177. [Crossref]
- Ministério da Saúde; *Manual de Vigilância e Controle da Leishmaniose Visceral*; Brasília, 2014. [Link] accessed in July 2024
- Ministério da Saúde; *Leishmaniose Visceral*; Brasília, 2021. [Link] accessed in July 2024
- Tiwari, N.; Gedda, M. R.; Tiwari, V. K.; Singh, S. P.; Singh, R. K.; *Mini-Rev. Med. Chem.* **2017**, *18*, 26. [Crossref]
- Winter, C.; Caetano, J. N.; Araújo, A. B. C.; Chaves, A. R.; Ostroski, I. C.; Vaz, B. G.; Pérez, C. N.; Alonso, C. G.; *Chem. Eng. J.* **2016**, *303*, 604. [Crossref]
- PASS filter online*, version 2.0; Way2Drug; Moscow, Russia, 2011.
- Goel, R. K.; Singh, D.; Lagunin, A.; Poroikov, V.; *Med. Chem. Res.* **2010**, *20*, 1509. [Crossref]
- MolPredictX, <https://www.molpredictx.ufpb.br/>, accessed in July 2024.
- Scotti, M. T.; Herrera-Acevedo, C.; Menezes, R.; Martin, H. J.; Muratov, E.; Silva, Á. Í. D. S.; Albuquerque, E. F.; Calado, L. F.; Coy-Barrera, E.; Scotti, L.; *Mol. Inf.* **2022**, *41*, 2200133. [Crossref]
- Maia, M. S.; Silva, J. P. R.; Nunes, T. A. L.; Sousa, J. M. S.; Rodrigues, G. C. S.; Monteiro, A. F. M.; Tavares, J. F.; Rodrigues, A. F.; Mendonça-Junior, F. J. B.; Scotti, L.; Scotti, M. T.; *Molecules* **2020**, *25*, 2281. [Crossref]
- Magalhães, T. B. S.; Silva, D. K. C.; Teixeira, J. S.; de Lima, J. D. T.; Barbosa-Filho, J. M.; Moreira, D. R. M.; Guimarães, E. T.; Soares, M. B. P.; *Front. Pharmacol.* **2022**, *13*, 846123. [Crossref]

31. Passos, C. L. A.; Ferreira, C.; Soares, D. C.; Saraiva, E. M.; *PLoS One* **2015**, *10*, e0141778. [Crossref]
32. *FlowJo*, version 10.6.1; Becton, Dickinson and Company, Ashland, OR, USA, 2017.
33. Research Collaboratory for Structural Bioinformatics, <https://www.rcsb.org/>, accessed in July 2024.
34. National Library of Medicine, <https://www.ncbi.nlm.nih.gov/genbank/>, accessed in July 2024.
35. European Molecular Biology Laboratory, <https://www.ebi.ac.uk/Tools/msa/clustalo/>, accessed in July 2024.
36. Bernstein, F. C.; Koetzle, T. F.; Williams, G. J. B.; Meyer, E. F.; Brice, M. D.; Rodgers, J. R.; Kennard, O.; Shimanouchi, T.; Tasumi, M.; *J. Mol. Biol.* **1977**, *112*, 535. [Crossref]
37. Waterhouse, A.; Bertoni, M.; Bienert, S.; Studer, G.; Tauriello, G.; Gumienny, R.; Heer, F. T.; de Beer, T. A. P.; Rempfer, C.; Bordoli, L.; Lepore, R.; Schwede, T.; *Nucleic Acids Res.* **2018**, *46*, 296. [Crossref]
38. Swiss-Model, <https://swissmodel.expasy.org/>, accessed in July 2024.
39. Protein Structure Validation Software Suite, http://psvs-1_5-dev.nesg.org/, accessed in July 2024.
40. Laskowski, R. A.; MacArthur, M. W.; Moss, D. S.; Thornton, J. M.; *J. Appl. Cryst.* **1993**, *26*, 283. [Crossref]
41. Lovell, S. C.; Davis, I. W.; Arendall, W. B.; de Bakker, P. I. W.; Word, J. M.; Prisant, M. G.; Richardson, J. S.; Richardson, D. C.; *Proteins: Struct., Funct., Bioinf.* **2003**, *50*, 437. [Crossref]
42. *Molegro Virtual Docker*, version 6.0.1; Molexus IVS, Denmark, 2024.
43. Thomsen, R.; Christensen, M. H.; *J. Med. Chem.* **2006**, *49*, 3315. [Crossref]
44. Abraham, M. J.; Murtola, T.; Schulz, R.; Páll, S.; Smith, J. C.; Hess, B.; Lindahl, E.; *SoftwareX* **2015**, *1*, 19. [Crossref]
45. *GROMACS*, version 2.1; Sphinx&Alabaster, Netherlands, 2022.
46. Bondi, A.; *J. Phys. Chem.* **1964**, *68*, 441. [Crossref]
47. *RBVI UCSF Chimera*; Chimera Commercial Licensing, California, USA, 2018.
48. Pettersen, E. F.; Goddard, T. D.; Huang, C. C.; Meng, E. C.; Couch, G. S.; Croll, T. I.; Morris, J. H.; Ferrin, T. E.; *Protein Sci.* **2021**, *30*, 70. [Crossref]
49. Nachbagauer, R.; Feser, J.; Naficy, A.; Bernstein, D. I.; Guptill, J.; Walter, E. B.; Berlanda-Scorza, F.; Stadlbauer, D.; Wilson, P. C.; Aydiillo, T.; *Nat. Med.* **2021**, *27*, 106. [Crossref]
50. Grace Development Team, <http://plasma-gate.weizmann.ac.il/Grace/>, accessed in July 2024.
51. *GraphPad Prism*, version 9.5.1; GraphPad Software, Boston, MA, USA, 2023.
52. Adinehbeigi, K.; Razi Jalali, M. H.; Shahriari, A.; Bahrami, S.; *Pathog. Global Health* **2017**, *111*, 176. [Crossref]
53. Rocha, V. P. C.; da Rocha, C. Q.; Queiroz, E. F.; Marcourt, L.; Vilegas, W.; Grimaldi, G. B.; Furrer, P.; Allémann, É.; Wolfender, J. L.; Soares, M. B. P.; *Molecules* **2018**, *24*, 1. [Crossref]
54. Zheoat, A. M.; Alenezi, S.; Elmahallawy, E. K.; Ungogo, M. A.; Alghamdi, A. H.; Watson, D. G.; Igoli, J. O.; Gray, A. I.; de Koning, H. P.; Ferro, V. A.; *Pathogens* **2021**, *10*, 175. [Crossref]
55. Gomes, A. N. P.; Camara, C. A.; Sousa, A. S.; Santos, F. A. R.; Santana Filho, P. C.; Dorneles, G. P.; Romão, P. R. T.; Silva, T. M. S.; *Rev. Bras. Farmacogn.* **2021**, *31*, 176. [Crossref]
56. Alonso, L.; Menegatti, R.; Gomes, R. S.; Dorta, M. L.; Luzin, R. M.; Lião, L. M.; Alonso, A.; *Eur. J. Med. Chem.* **2020**, *151*, 105407. [Crossref]
57. Nardella, F.; Gallé, J. B.; Bourjot, M.; Weniger, B.; Vonthron-Sénécheau, C. In *Natural Antimicrobial Agents*; Springer International Publishing: Cham, 2018, p. 163. [Crossref]
58. Ortalli, M.; Ilari, A.; Colotti, G.; De Ionna, I.; Battista, T.; Bisi, A.; Gobbi, S.; Rampa, A.; Di Martino, R. M. C.; Gentilomi, G. A.; Varani, S.; Belluti, F.; *Eur. J. Med. Chem.* **2018**, *152*, 527. [Crossref]
59. Oprea, T. I. In *Chemoinformatics in Drug Discovery*; Oprea, T. I., ed.; Wiley: Germany, 2005, p. 43-57. [Crossref]
60. Cruz, J. H. D. A.; Moreira, I. C. D. S.; Alves, M. D. F. V.; Oliveira, H. M. B. F. D.; Oliveira Filho, A. A. D.; Alves, M. A. S. G.; *Arch. Health Invest.* **2020**, *8*, 674. [Crossref]
61. Surabhi, S.; Singh, B.; *J. Drug Delivery Ther.* **2018**, *8*, 504. [Crossref]
62. Yu, W.; MacKerell, A. D. In *Antibiotics Methods and Protocols*; Sass, P., ed.; Tübingen, Germany, 2016, p. 85. [Crossref]
63. de Mello, M. V. P.; Abraham-Vieira, B. D. A.; Domingos, T. F. S.; de Jesus, J. B.; de Sousa, A. C. C.; Rodrigues, C. R.; Souza, A. M. T. D.; *Eur. J. Med. Chem.* **2018**, *150*, 920. [Crossref]
64. N'guessan, D. U. J. P.; Alzain, A. A.; Adouko, E. M.; *J. Appl. Pharm. Sci. Res.* **2021**, *4*, 18. [Crossref]
65. Osman, M. S.; Awad, T. A.; Shantier, S. W.; Garenalbi, E. A.; Osman, W.; Mothana, R. A.; Nasr, F. S.; Elhag, E. R.; *Arabian J. Chem.* **2022**, *15*, 103717. [Crossref]
66. Tolosa, L.; Donato, M. T.; Gómez-Lechón, M. J.; *Methods in Molecular Biology*; Springer: New York, 2014, p. 333.
67. Costa, C. A.; Lopes, R. M.; Ferraz, L. S.; Esteves, G. N. N.; Di Iorio, J. F.; Souza, A. A.; de Oliveira, I. M.; Manarin, F.; Judice, W. A. S.; Stefani, H. A.; Rodrigues, T.; *Bioorg. Med. Chem.* **2020**, *28*, 115511. [Crossref]
68. Zhang, S.; Li, T.; Zhang, Y.; Xu, H.; Li, Y.; Zi, X.; Yu, H.; Li, J.; Jin, C. Y.; Liu, H. M.; *Toxicol. Appl. Pharmacol.* **2016**, *309*, 77. [Crossref]
69. Sinha, S.; Batovska, D. I.; Medhi, B.; Radotra, B. D.; Bhalla, A.; Markova, N.; Sehgal, R.; *Malaria J.* **2019**, *18*, 421. [Crossref]
70. Escrivani, D. O.; Charlton, R. L.; Caruso, M. B.; Burle-Caldas, G. A.; Borsodi, M. P. G.; Zingali, R. B.; Arruda-Costa, N.; Pameira-Mello, M. V.; Jesus, J. B.; Souza, A. M. T.; Abraham-Vieira, B.; Freitag-Pohl, S.; Pohl, E.; Steel, P. G.; *PLoS Neglected Trop. Dis.* **2021**, *15*, e0009951. [Crossref]

71. Bello, M. L.; Chiaradia, L. D.; Dias, L. R. S.; Pacheco, L. K.; Stumpf, T. R.; Mascarello, A.; Steindel, M.; Yunes, R. A.; Castro, H. C.; Nunes, R. J.; Rodrigues, C. R.; *Bioorg. Med. Chem.* **2011**, *19*, 5046. [Crossref]
72. Santiago-Silva, K. M.; Bortoleti, B. T. S.; Oliveira, L. N.; Maia, L. F. A.; Castro, J. C.; Costa, I. C.; Lazzarin, D. B.; Wardell, J. L.; Wardell, S. M. S. V.; Albuquerque, M. G.; Lima, C. H. S.; Pavanelli, W. R.; Bispo, M. L. F.; Gonçalves, R. S. B.; *Antibiotics* **2022**, *11*, 1402. [Crossref]
73. Jitareanu, A.; Tataringa, G.; Zbancioc, A. M.; Trifan, A.; *Medical-Surgical J.* **2018**, *122*, 3. [Crossref]
74. Ministério da Saúde; *Manual de Leishmaniose Tegumentar*; Brasília, 2017. [Link] accessed in July 2024
75. Vasconcelos, J. M.; Gomes, C. G.; Sousa, A.; Teixeira, A. B.; Lima, J. M.; *Rev. Bras. Anal. Clin.* **2018**, *50*, 221. [Crossref]
76. Kong, L.; Ju, F.; Zheng, W.; Zhu, J.; Sun, S.; Xu, J.; Bu, D.; *J. Comput. Biol.* **2022**. [Crossref]
77. Gao, M.; Skolnick, J.; *Bioinformatics* **2021**, *27*, 490. [Crossref]
78. Fu, Y.; Zhao, J.; Chen, Z.; *Computational and Mathematical Methods in Medicine* **2018**, 2018, ID 3502514. [Crossref]
79. Pinzi, L.; Rastelli, G.; *Int. J. Mol. Sci.* **2019**, *20*, 4331. [Crossref]
80. Fan, J.; Fu, A.; Zhang, L.; *Quant. Biol.* **2019**, *7*, 83. [Crossref]
81. Zhang, X.; Stevens, R. C.; Xu, F.; *Trends Biochem. Sci.* **2015**, *40*, 2. [Crossref]
82. Tripathi, M. K.; Ahmad, S.; Tyagi, R.; Dahiya, V.; Yadav, M. K.; In *Computer Aided Drug Design (CADD): From Ligand-Based Methods to Structure-Based Approaches*; Rudrapal, M.; Egbuna, C., eds.; Elsevier, 2022, ch. 5. [Crossref]
83. Yan, B. X.; Sun, Y. Q.; *J. Biol. Chem.* **1997**, *272*, 6. [Crossref]

Submitted: March 6, 2024

Published online: July 23, 2024